Measurement of One- and Two-Electron-Loss Cross Sections for He^- Ions in H_2, He, and Ne Gases (400-1500 keV)

G. Ryding, A. B. Wittkower, and P. H. Rose
R. J. Van de Graaff Laboratory, High Voltage Engineering Corporation, Burlington, Massachusetts
(Received 13 May 1968)

The destruction of He^- ions during passage through H_2, He, and Ne gas targets has been studied in the range of impact energies 400–1500 keV. He^- ions were formed by the charge exchange of positive He^+ ions. The cross sections for the loss of one (σ_{-10}) and two (σ_{-11}) electrons were determined from the rate of growth of the fast collision products He^0 and He^+ with increasing target gas density.

INTRODUCTION

The charge-changing collision cross sections σ_{ij} for the light projectiles of helium have been the subject of numerous investigations.[1] A large fraction of these reports are concerned with the incident projectiles He^{++}, He^+, and He^0. Up to the present time charge-changing cross sections for He^- projectiles have only been measured at energies below 70 keV.[2,3] In the present work relative cross sections have been measured at higher energies by observing the growth of fast He^0 and He^+ collision products with increasing target thickness. These relative values are standardized to the previously determined absolute single electron-capture cross section (σ_{10}) for protons in hydrogen at 1 MeV.[4-6]

EXPERIMENTAL APPROACH

A schematic diagram of the apparatus is shown in Fig. 1. A monoenergetic, mass-analyzed beam of He^+ ions from a Van de Graaff accelerator entered the charge exchange canal. This consisted of a 0.1-in. diam tube 3 in. long into which gas was admitted by means of a needle valve. The beam emerging from the canal was collimated by a small aperture A_1 (0.006 in. diam) and then separated into the charge components He^{++}, He^+, He^0, and He^- by the first pair of electrostatic deflector plates. The deflection also directed the small He^- fraction along the axis of the target gas cell. This gas cell was 1.0 in. long with entrance (A_2) and exit (A_3) apertures 0.040 and 0.050 in. diam, respectively.

The flow of target gas to the cell was regulated by a fine control needle valve and the flow rate was measured by means of a diaphragm-type differential pressure gauge.[7] This gauge recorded the pressure drop P produced by the molecular flow of gas through a low-conductance aperture in the gas feed line. Under these conditions the target thickness π in the gas cell is given by

$$\pi = KP, \tag{1}$$

where K is a constant independent of the gas introduced. Gas escaping from the cell was removed by a 400-liter/sec diffusion-pump system which maintained a pressure below 7×10^{-7} Torr at all times.

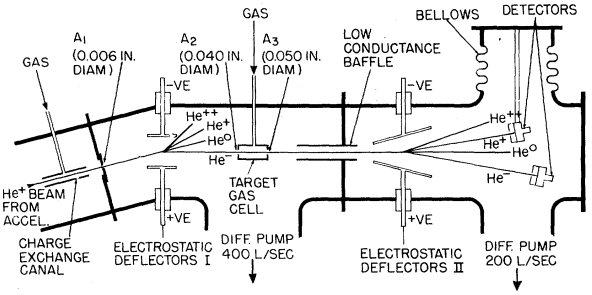

FIG. 1. Experimental apparatus.

The beam emerging from the gas cell passed into the analysis chamber, where it was again separated into the components He^{++}, He^+, He^0, and He^- by the second pair of deflector plates. The analysis region was independently pumped by a 200-liter/sec diffusion-pump system and the low-conductance baffle between the gas cell and analysis chambers enabled pressures below 2×10^{-7} Torr to be maintained in this region at all times. The low base pressures in the system ($\sim 10^{-7}$ Torr) minimized beam interaction with residual gases and the signals arising from such interactions were always small compared to the observed signals. Two silicon surface barrier detectors were used to detect the fast-beam components. A fixed detector monitored the primary He^- beam and a movable detector mounted on a vacuum bellows could be tracked across the beams to locate either the He^0, He^+, or He^{++} components. Suitable primary-beam count rates of $10^4 - 10^5$ per sec were chosen by regulating the intensity of the He^+ beam from the accelerator and the flow of gas to the charge-exchange canal.

The beam collimating and gas-cell apertures A_1, A_2, and A_3 were aligned on the beam axis using a microalignment telescope accurate to 0.001 in. This enabled the primary He^- beam ($\sim$ 0.006 in. diam) to pass through the gas cell without striking the apertures A_2 (0.040 in. diam) and A_3 (0.050 in. diam). Consequently problems associated with stripping, scattering, and energy loss on aperture edges were eliminated. The absence of these unwanted effects was confirmed by low residual signals and monoenergetic detector-output spectra observed using a multichannel pulse-height analyzer. The geometry of the detectors and the beam apertures ensured that all particles scattered

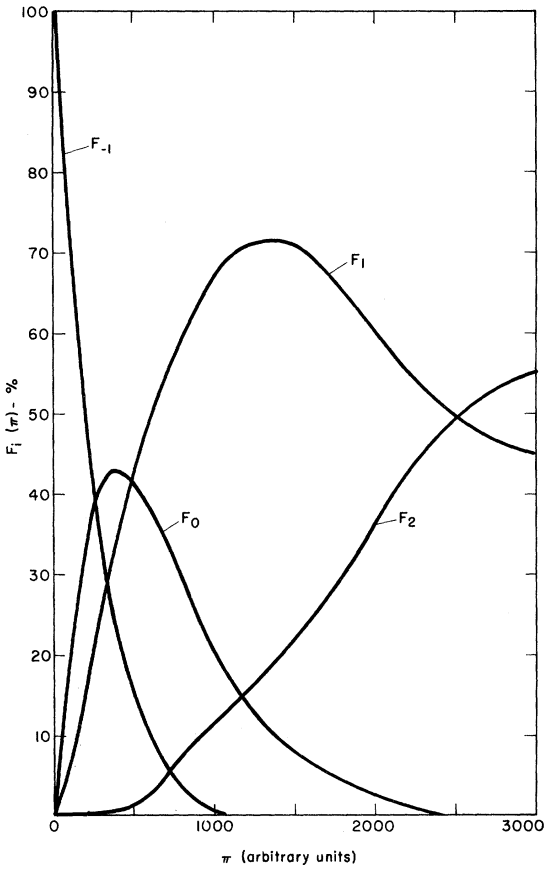

FIG. 2. Variations of the He^-, He^0, He^+, and He^{++} fractions as a function of target thickness (π) for He^- ions in H_2 at 1350 keV.

through angles less than 3 mrad were detected with 100% efficiency. Flat top characteristics of each detector signal as a function of either detector position or deflector-plate voltage confirmed that particles scattered through greater angles in both thin and thick targets constituted a negligible fraction of the beam.

The variations of the He^-, He^0, He^+, and He^{++} signals were studied as a function of target-gas thickness. Figure 2 summarizes a typical study for He^- in H_2 at 1350keV and shows the beam fractions approaching equilibrium values. According to Allison,[1] the growth of a component with charge i as a function of target thickness π is given by

$$F_i(\pi) = \sum a_n \pi^n , \qquad (2)$$

where the a_n are constants and $F_i(\pi)$ is the fraction of the total beam in charge state i.

For very thin targets, when multiple collisions may be ignored, the terms with $n > 1$ can be neglected and the coefficient a_1 is the cross section for charge transfer directly to charge state i. For somewhat thicker targets the He^0 and He^+ fractions of the beam are therefore given by

$$F_0(\pi) \simeq \sigma_{-10}\pi + a_2\pi^2 \qquad (3)$$

and $$F_1(\pi) \simeq \sigma_{-11}\pi + a_2'\pi^2 , \qquad (4)$$

where a_2 and a_2' are constants involving the various cross sections.

Investigations were conducted using low target-gas densities and relative cross sections values (σ_{-10} and σ_{-11}) were determined from the initial slope of the fast He^0 and He^+ growth curves. Typical growth curves are shown in Fig. 3.

At the higher-target gas pressures, conditions for single collisions were not always satisfied in the production of fast He^+ ions, and the growth curves became nonlinear. Consequently the initial slope of the curve was determined by fitting the quadratic function of Eq. (4) to the data using the method of least squares. For comparison the slope was also determined by fitting a straight line to the low-pressure data in the region that appeared to be linear. In spite of the small random scatter of the data points, it was not always possible to judge at which region of the growth curve the term in π^2 became significant and the curve became nonlinear. As a result the quoted values obtained by the quadratic method were from 2–13% lower than those derived from the apparent linearity of the growth curve near the origin. In the case of the He^0 growth curve the quadratic coefficient a_2 [Eq. (3)] was found to be negligible and the initial slopes were obtained by fitting a straight line to the data points.

In order to standardize the relative cross sections obtained in this way, the relative cross section for single electron capture (σ_{10}) by protons in hydrogen at 1 MeV was measured. This was accomplished by replacing the fixed detector with a

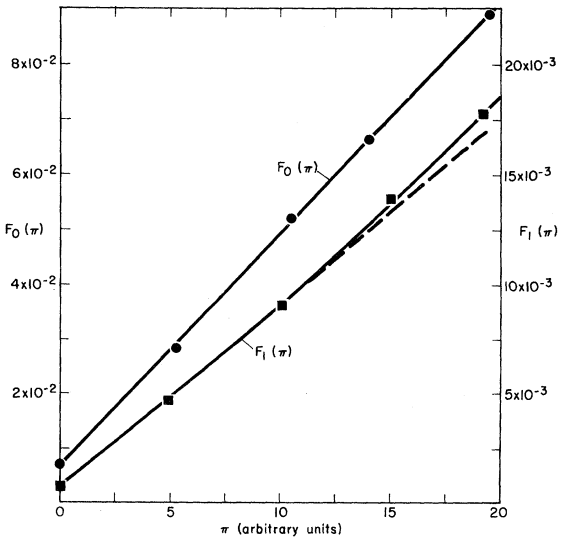

FIG. 3. Growth of the He^0 fraction (F_0) and the He^+ fraction (F_1) as a function of target thickness (π) for He^- ions in Ne at 1150 keV.

TABLE I. Cross sections σ_{-10} and σ_{-11} for He^- in H_2, He, and Ne as a function of energy. (Units of 10^{-17} cm^2/atom.)

Energy (keV)	σ_{-10} H_2	σ_{-10} He	σ_{-10} Ne	σ_{-11} H_2	σ_{-11} He	σ_{-11} Ne
400	26.0±1.0	29.7±1.2	59.1±2.4	1.80±0.23	3.07±0.24	6.65±0.40
600	20.6±0.8	22.1±0.9	54.2±2.2	1.75±0.23	2.60±0.21	7.72±0.46
800	16.8±0.7	18.9±0.8	47.8±1.9	1.89±0.37	2.20±0.19	7.12±0.43
1000	14.6±0.6	16.5±0.7	44.9±1.8	1.66±0.22	2.35±0.19	8.43±0.50
1150	13.9±0.6	14.5±0.6	41.9±1.7	...	2.30±0.18	7.77±0.47
1350	11.7±0.5	12.3±0.5	38.2±1.5	1.03±0.13	2.21±0.18	6.75±0.40
1500	11.7±0.5	10.5±0.4	...	1.24±0.16	2.04±0.16	...

Faraday cup in order to monitor the primary proton beam. The growth of fast H^0 atoms with increasing target thickness was then studied by means of the movable silicon surface-barrier detector. The relative cross section obtained in this way was normalized to previously determined absolute values.[4-6] The reported values are as follows (units of 10^{-22} cm^2/molecule):

5.2 Barnett and Reynolds[4]

4.8 (Interpolated between 851 and 1063 keV) Welsh *et al.*[5]

1.0 Williams[6]

A value of 5.0×10^{-22} cm^2/molecule was assumed and the constant K (Eq. 1) was deduced from the slope of the H^0 growth curve. Since the value of K is independent of target-gas type, cross-section values σ_{-10} and σ_{-11} for He^- in H_2, He, and Ne could then be calculated.

RESULTS

The cross-section values obtained are listed in Table I and shown in Figs. 4 and 5. The indicated random errors were estimated from the most probable error in the method of least-squares fitting and from the repeatability of the data points. The systematic error involved in the standardization procedure is not included and errors involved in the determination of the ion-beam energy are negligible.

In the range of energies studied, the single elec-

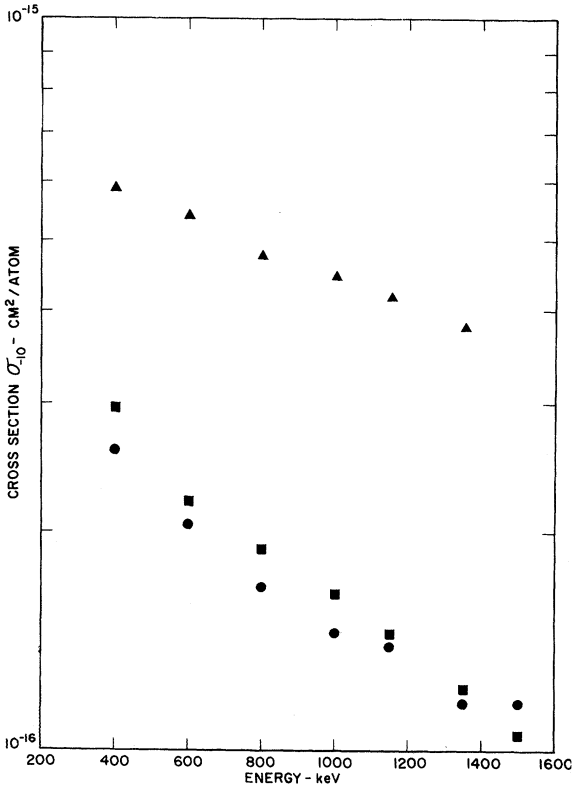

FIG. 4. Cross sections for the loss of one electron (σ_{-10}) for He^- ions in H_2, He, and Ne as a function of He^- ion energy. ●, H_2. ■, He. ▲, Ne.

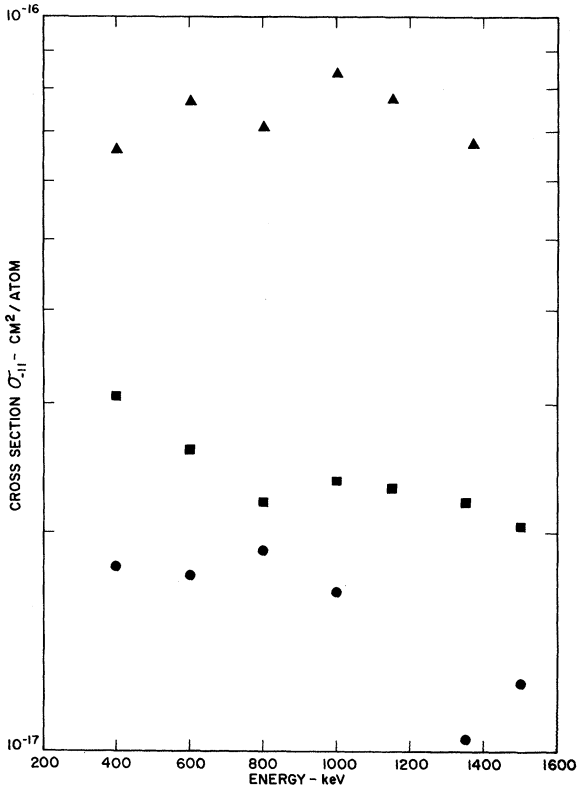

FIG. 5. Cross sections for the loss of two electrons (σ_{-11}) for He^- ions in H_2, He, and Ne as a function of He^- ion energy. ●, H_2. ■, He. ▲, Ne.

tron-loss cross sections (σ_{-10}) decrease monotonically with increasing energy and in general increase with the atomic number, Z, of the target. This is consistent with the findings of Nikolaev[8] for $Z < 18$. The two electron-loss cross sections (σ_{-11}) also increase with the atomic number, Z, of the target but only vary slowly with energy.

ACKNOWLEDGMENTS

The authors are indebted to P. H. Trent, for assistance in the numerical analysis of data and to our accelerator engineer, W. M. Powers.

[1]S. K. Allison and M. Garcia-Munoz, Atomic and Molecular Processes, edited by D. R. Bates (Academic Press Inc., New York 1962), Chap. 19.
[2]D. J. Nicholas, C. W. Trowbridge, and W. D. Allen, Phys. Rev. 167, 38 (1968).
[3]P. M. Windham, P. J. Joseph, and J. A. Weinman, Phys. Rev. 109, 1193 (1958).
[4]C. F. Barnett and H. K. Reynolds, Phys. Rev. 109, 355 (1958).
[5]L. M. Welsh, K. H. Berkner, S. N. Kaplan, and R. V. Pyle, Phys. Rev. 158, 85 (1967).
[6]J. F. Williams, Phys. Rev. 157, 97 (1967).
[7]M. K. S. Instruments, Inc., Baratron Model 77H-3.
[8]V. S. Nikolaev, Usp. Fiz. Nauk 00, 000 (1965) [English transl.: Soviet Phys. – Usp. 8, 269 (1965)].

PHYSICAL REVIEW VOLUME 174, NUMBER 1 5 OCTOBER 1968

Electronic Transitions in Slow Collisions of Atoms and Molecules. I.*

Joseph C. Y. Chen
Department of Physics and Institute for Pure and Applied Physical Sciences, University of California, San Diego, La Jolla, California

and

Kenneth M. Watson†
Institute of Geophysics and Planetary Physics, University of California, San Diego, La Jolla, California

(Received 28 March 1968)

The semiclassical approximation is systematically applied to the study of electronic transitions in near-adiabatic collisions of atoms and molecules. The use of the eikonal approximation permits the coupled equations of scattering theory to be reduced to one-dimensional equations defined along classical trajectories. The theory for rearrangement collisions is developed into a form appropriate for use with the eikonal description of heavy-particle motion.

I. INTRODUCTION

In this paper we study the theory of electronic transitions in the collisions of slow atoms and molecules (for brevity, we shall refer to the particles as "atoms"). The conditions assumed will be such that the motion of the atomic centers of mass is essentially classical. Our goal is to systematically extract the possible approximations arising from this classical aspect of the problem.

Stationary-state scattering theory will be used. The state function will be expanded in terms of *adiabatic states* – often called "perturbed stationary states." We shall use the eikonal approximation for the coefficients in this expansion, which describe the motion of the atomic mass centers.[1]

Except when there are degeneracies, electronic transitions occur only for finite collision velocities (the adiabatic theorem). We shall use the term "near-adiabatic" to refer to transitions that occur at low velocities.

The formulation of the "perturbed stationary-state" method for cases in which rearrangement does not occur is well-known. We briefly review this in Sec. II, expressing it in a form suitable for our application. When rearrangement occurs, the problem is much more subtle. Discussions have been given in the context of time-dependent perturbation theory, for example, by Bates and McCarroll[2] and by Mittleman.[3] Thorson[4] has observed that the adiabatic (or Born-Oppenheimer) states of the perturbed stationary-state method do not lead to correct asymptotic incoming or outgoing states. He proposes an approximation scheme consistent with this formal requirement of scattering theory (a point previously ignored). In Sec. III and Appendix B we give a formulation for rearrangement collision that is consistent with formal scattering theory and with the eikonal approximation.